Epidemics 42 (2023) 100672

Contents lists available at ScienceDirect

Epidemics

journal homepage: www.elsevier.com/locate/epidemics

A novel method to jointly estimate transmission rate and decay rate parameters in environmental transmission models

You Chang *, Mart C.M. de Jong

Quantitative Veterinary Epidemiology Group, Wageningen Institute of Animal Sciences, the Netherlands

ARTICLE INFO

Keywords:
Transmission models
Pathogen decay
Stochastic simulation
Exposure-based estimation

ABSTRACT

In environmental transmission, pathogens transfer from one individual to another via the environment. It is a common transmission mechanism in a wide range of host-pathogen systems. Incorporating environmental transmission in dynamic transmission models is crucial for gauging the effect of interventions, as extrapolating model results to new situations is only valid when the mechanisms are modelled correctly. The challenge in environmental transmission models lies in not jointly identifiable parameters for pathogen shedding, decay, and transmission dynamics. To solve this unidentifiability issue, we present a stochastic environmental transmission model with a novel scaling method for shedding rate parameter and a novel estimation method that distinguishes transmission rate and decay rate parameters. The core of our scaling and estimation method is calculating exposure and relating exposure to infection risks. By scaling shedding rate parameter, we standardize exposure to pathogens contributed by one infectious individual present during one time interval to one. The standardized exposure leads to a standard definition of transmission rate parameter applicable to scenarios with different decay rate parameters. Hence, we unify direct transmission (large decay rate) and environmental transmission in a continuous manner. More importantly, our exposure-based estimation method can correctly estimate back the transmission rate and the decay rate parameters, while the commonly used trajectory-based method failed. The reason is that exposure-based method gives the correct weight to infection data from previous observation periods. The correct estimation from exposure-based method will lead to more reliable predictions of intervention impact. Using the effect of disinfection as an example, we show how incorrectly estimated parameters may lead to incorrect conclusions about the effectiveness of interventions. This illustrates the importance of correct estimation of transmission rate and decay rate parameters for extrapolating environmental transmission models and predicting intervention effects.

1. Introduction

In many infectious diseases, pathogens are shed into the environment on surfaces, in water, in air, etc. Pathogens persist there, and subsequently infect individuals that are exposed to the contaminated environment. This is called environmental transmission. A wide range of human and animal infections are transmitted via the environment (Breban, 2013; Chen et al., 2013; Lanzas et al., 2020; Li et al., 2009). For example, cholera, rotavirus, norovirus, *Campylobacter jejuni*, enterotoxigenic *Escherichia coli*, bovine tuberculosis, foot and mouth disease and Hepatitis E virus can transmit via contaminated environment such as water, food, surfaces, urine, faeces etc. (Allen et al., 2021; Ashbolt, 2004; Bouwknegt et al., 2008; de Rueda et al., 2015; Van der Poel, 2014). Respiratory infections, such as influenza, rhinovirus and SARS-CoV2 can be transmitted when an infectious person exhales virus particles to aerosols, droplets, which can be taken up by other individuals (either directly from the air or via fomites) (Kraay et al., 2021; Weber and Stilianakis, 2008; Winther et al., 2007). The existence of various environmental transmission routes makes it important for us to understand better environmental transmission dynamics.

Mathematical models can be constructed to understand the underlying transmission dynamics and then be used to predict the effects of intervention strategies (De Jong, 1995; Grassly and Fraser, 2008). In addition, models can also be extrapolated to scenarios where future transmission conditions are different due to environmental changes. We need accurate predictions if we want to be prepared for new situations

* Correspondence to: Quantitative Veterinary Epidemiology Group, Wageningen Institute of Animal Sciences, Wageningen University & Research, P.O. Box 338, 6700 AH Wageningen, the Netherlands.
E-mail address: you.chang@wur.nl (Y. Chang).

https://doi.org/10.1016/j.epidem.2023.100672
Received 4 May 2022; Received in revised form 23 December 2022; Accepted 26 January 2023
Available online 2 February 2023

and take measures to mitigate the possible effects. Several quantification approaches have been used for this purpose, such as the well-established risk factors analysis and dynamic models (Woolhouse, 2011).

Relative risk analysis finds associations between interventions and the risk of infection assuming the same exposure in a reference population and an intervention population. Relative risks can provide some insight into the efficacy of interventions (Aiello et al., 2008; Cairncross et al., 2010; Liang et al., 2020). However, the magnitude of the impact cannot be extrapolated to other situations or populations where the exposure is different, as the relationship between exposure and infection probability is not linear (Bijma et al., 2022; Halloran et al., 1999; Kermack and McKendrick, 1927; Teunis and Havelaar, 2000; Turner., 1975). Therefore, dynamics modelling is often preferred over risk factor analysis when predicting future risks (Woolhouse, 2011).

However, there are challenges in dynamic modelling for environmental transmission. Environmental contamination is usually unobserved or observed under lab circumstances, which may differ from the normal circumstances of pathogen transmission. In the absence of correct and detailed environmental contamination data, the shedding rate, decay rate, and transmission rate parameters are structurally not jointly identifiable (Brouwer et al., 2018; Eisenberg et al., 2013). For example, a certain rate of infection can be the result of a lower transmission rate parameter per pathogen with more pathogens in the environment or of a higher transmission rate parameter per pathogen with fewer pathogens. Measuring environmental data or the rates of shedding or decay processes via experiments have been suggested to help this unidentifiability issue (Brouwer et al., 2018, 2017; Eisenberg et al., 2013). However, environmental data measurements and experiments can be expensive, unethical when involving pathogen challenging, and the natural inoculation is usually different from experimental inoculation.

Another challenge is the lack of a suitable estimation method for quantifying environmental transmission. A widely used estimation method is based on fitting observed infection data to the trajectories simulated by ordinary differential equation (ODE) models (Brouwer et al., 2017; Eisenberg et al., 2013; Erazo et al., 2021; Towers et al., 2018), which we call trajectory-based estimation. The underlying mathematical models of this estimation are easy to build, and one can add complexity in transmission mechanisms with different routes (Li et al., 2009). However, a recent simulation study (Lee et al., 2017) shows that models with different mechanisms can have similar fits, making it impossible to distinguish the model with the correct transmission mechanisms from other models.

In contrast, another quantification method estimates transmission rate parameters based on linking exposure to infection probability. This exposure-based method has been used both in quantifying direct transmission (Dekker et al., 2020; Eblé et al., 2019; Velthuis et al., 2002) and indirect transmission (Biemans et al., 2018; Corbett et al., 2019; de Rueda et al., 2015; Velkers et al., 2012). Bootsma et al. (2007) has attempted to apply this exposure-based method for environmental transmitted infection in hospitals but had difficulties in reconstructing the history of the exposure to infectious individuals. Here we postulate that adapting this exposure-based estimation method to environmental transmission would be challenging, but promising.

Therefore, the main objective of our paper is to solve the not jointly identifiable issue when quantifying environmental transmission. We start out by building a stochastic environmental transmission model with a novel scaling method. Then, we present our novel estimation method for environmental transmission by adapting the exposure-based estimation. In order to evaluate exposure-based estimation method and compare with the trajectory-based estimation, we analysed simulated infection data using our stochastic environmental model. We illustrate our newly developed model with a case study on the prediction of the impact of disinfection on environmental transmission. This shows the importance of correctly estimating parameters for drawing correct conclusions on the effect of interventions, and more generally, for extrapolation transmission model results.

2. Models and results

In this section, we will first explain the environmental transmission model framework (1.1) and present a novel scaling method for shedding rate by standardizing exposure (1.2). The model will then be applied to simulate a time series of infection data (1.3). Then, the simulated data will be analysed by two different statistical methods (exposure-based and trajectory-based) to assess whether they can estimate back decay rate and transmission rate parameters (1.4). Furthermore, the robustness of the exposure-based estimation method will be tested by sensitivity analysis (1.5). In the end, we will explore the application of the environmental transmission model by predicting the impact of disinfection (1.6).

2.1. Environmental transmission model

We adopted a stochastic SIS stochastic compartmental model with an extra environment compartment (Fig. 1). Infections are assumed to occur through the environmental compartment only.

We model in continuous time t with discrete individuals. Thus, (S_t,I_t) are discrete numbers of susceptible and infectious individuals. (S_t,I_t) make discrete jump to (S_t+1,I_t-1) for recovery at rate $\beta\frac{E(t)}{N}S_t$ and to (S_t-1,I_t+1) for infection at rate αI_t. In the interval between these events, the (S_t,I_t) population state does not change. In contrast, $E(t)$ is a continuous variable for environmental contamination in continuous time. To distinguish continuous from discrete variables, we use the subscript notation for time t for discrete variables (S_t and I_t, both in continuous time), and the parentheses notation for the continuous variable $E(t)$..

In each interval between any two sequential state transitions $t\in(t1,t2)$, the number of infectious individuals (I_t) during the interval is determined as I_{t1} and is constant. Remember that the interval ends when I_t changes to I_{t2}. During the interval, the infectious individuals I_{t1} shed pathogens in the environment at constant rate φI_{t1} and in the environment pathogens decay with a changing rate $\mu E(t)$. These two processes during each interval between state transitions $(t1,t2)$ are modelled deterministically because of the large number of pathogens in the environment:

$$\frac{dE(t)}{dt}=\varphi I_{t1}-\mu E(t) \tag{1}$$

where μ is pathogens' decay rate parameter, i.e. the rate at which viable pathogens become inactivated or removed from the environment, and φ

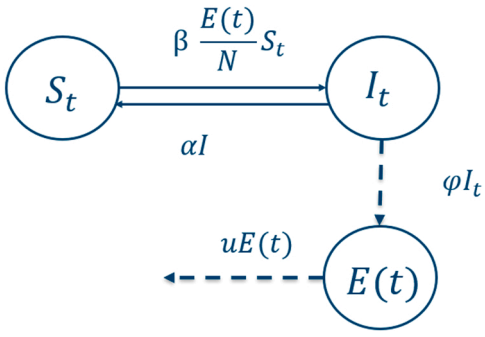

Fig. 1. A schematic representation of the stochastic SIS model with transmission through the environment. S_t,I_t represent susceptible, infectious compartments and $E(t)$ represents the environmental compartment. The solid lines represent the flow of individuals (stochastic discrete jumps) to another state. The transmission from S_t to I_t occurs at rate $\beta\frac{E(t)}{N}S_t$ and the transition from I_t to S_t occurs at rate αI_t. The dotted lines represent the flow of pathogens in the environment, modelled as deterministic processes, φI_t represents the shedding rate at which infectious individuals shed pathogens into environment and $\mu E(t)$ represents the decay rate at which pathogens decay in the environment.

is the shedding rate parameter, i.e. the rate at which pathogens are added to the environment by each infectious individual during the interval. When starting from a clean environment with *one* infectious individual present, the environmental contamination increases with time and reaches a plateau when the shedding rate in the population equals the decay rate of environmental pathogens ($E(equilibrium) = \frac{\varphi}{\mu}$). If the infectious individual is recovered or removed, environmental contamination decreases exponentially with time: $E(t) = e^{-\mu(t-t_{equilibrium})}E(equilibrium)$ (Fig. 2).

The state transitions (solid lines in Fig. 1) are modelled by a continuous-time discrete-state Markov process via Gillespie's Direct Method (Gillespie, 1977). The detailed algorithm of simulation is given in Section 2.3.

We calculate the basic reproduction number R for this environmental model. The ordinary differential equation of the model in Fig. 1 can be written as:

$$\frac{dE}{dt} = \varphi I - \mu E, \frac{dI}{dt} = \frac{\beta ES}{N} - \alpha I, \frac{dS}{dt} = -\frac{\beta ES}{N} + \alpha I.$$

We obtain the Next Generation Matrix from the transmission matrix (T) and transition matrix (Σ) using I and E as the two states in that order (Diekmann et al., 2010):

$$T = \begin{bmatrix} 0 & \beta \\ 0 & 0 \end{bmatrix}, \Sigma = \begin{bmatrix} -\alpha & 0 \\ \varphi & -\mu \end{bmatrix},$$

The reproduction ratio is thus the largest eigenvalue of $-T\Sigma^{-1}$, hence $R = \frac{\beta\varphi}{\alpha\mu}$.

We can also calculate the R of the stochastic model (Fig. 1) from biological interpretation by determining: 1) how long an infectious individual stay infectious (expected value of t); 2) how long environmental contamination stays in the environment (exponential decay with μ); 3) how many pathogens are shed into environment by an infectious individual per time unit (φ); 4) how many individuals are expected to be infected per unit of environmental contamination per time unit (β). From that it follows that, $R = \int_0^\infty \int_0^\infty \varphi\beta e^{-\mu x}\alpha t e^{-\alpha t} dx dt = \frac{\beta\varphi}{\alpha\mu}$.

2.2. Scaling the shedding rate parameter

The shedding rate parameter φ and the transmission rate parameter β are not structurally jointly identifiable from infection data (Brouwer et al., 2018). Therefore, the shedding rate is usually scaled to unity or another fixed value (Nixon et al., 2021; Rohani et al., 2009; Widgren et al., 2018).

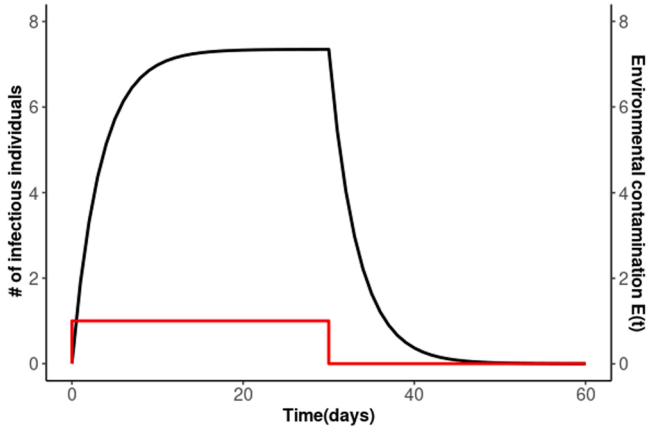

Fig. 2. An example showing the discrete jumps in I_t and continuous changes in $E(t)$. The red line represents I_t jumping first from 0 to 1 and then later from 1 to 0 and the black line represents the $E(t)$ resulting from that. Environmental contamination builds up till equilibrium and decays after removal of the infectious individual.

However, choosing a fixed value for the shedding rate parameter φ makes it difficult to interpret the transmission rate parameter β among different decay rate parameter μ. For example, the environmental contamination and the exposure to environmental contamination during an interval become lower and lower with increasing values of the decay rate parameter μ. The transmission rate parameters β is estimated by fitting the exposure to a dose-response curve based on an observed infection probability ($P = 1 - e^{(-\beta * exposure)}$). Consequently, when decay rate is large and the exposure is low, the estimates of the transmission rate parameters β have to increase proportionally when a certain infection probability is observed. This relationship between β and μ can be seen in the basic reproduction rate ($R = \frac{\beta}{\alpha\mu}$ when $\varphi = 1$). When μ is close to infinity, β is also close to infinity which is hard to interpret because the ratio between β and μ is not infinite. In reality, transmission with a large decay rate parameter μ is seen as direct transmission, with the basic reproduction ratio as $R = \frac{\beta}{\alpha}$. The interpretation of β is incomparable among transmission with different μ, which creates a sharp distinction between direct and environmental transmission.

Therefore, we propose a scaling method that generates a consistent interpretation of β. This is inspired by our work on experimental transmission where often the probability of infection is observed (Corbett et al., 2019; de Rueda et al., 2015; Velkers et al., 2012). In an imagined transmission experiment, susceptible individuals are put in a clean environment with infectious individuals. Susceptible individuals get exposed to pathogens shed by infectious individuals. The infection status of susceptible individuals is observed in an interval (e.g., a day in the following text), from which the probability of infection can be calculated. This probability is a certain value, despite whether susceptible individuals get exposed directly during close contact or indirectly via environment. In fact, this probability is dependent on the total exposure during a day and the transmission rate parameter ($P = 1 - e^{(-\beta * exposure)}$). During the first day of the experiment, the exposure is a fixed value among different transmission mechanism assumptions because of no historic environmental contamination. The total exposure to one infectious individual during a day starting with no historic contamination is represented as 1 in direct transmission, while as $\int_0^1 E(t)dt$ when assuming an environmental transmission. Therefore, we standardize the exposure to environmental contamination shed by one infectious individual during a day to one unit, which generates a consistent interpretation of transmission rate parameter among different transmission mechanism assumptions.

We firstly solve Eq. (1) to derive the environmental contamination for every time point $(t1 + \tau)$ within an interval $(t1, t2)$, where $t1$, $t2$ represent any two sequential time points at which transition events occur:

$$E(t1 + \tau|, I_{t1}, E(t1)) = \frac{(1 - e^{-\tau\mu})}{\mu}\varphi I_{t1} + e^{-\tau\mu}E(t1). \quad (2)$$

I_{t1} and $E(t1)$ are the number of infectious individuals and environmental contamination, respectively, at the start of the interval, the time point $t1$ (i.e., at the moment at which the latest transition occurred). The total exposure to the environmental contamination during $(t1, t1 + \tau)$ is then the integral of Eq. (2) as:

$$\int_{t1}^{t1+\tau} E(t|, I_{t1}, E(t1))dt = \frac{(-1 + e^{-\mu\tau} + \mu\tau)}{\mu^2}\varphi I_{t1} + \frac{1 - e^{-\mu\tau}}{\mu}E(t1). \quad (3)$$

The exposure consists of two parts; the exposure to the environmental contamination shed by I_{t1} during $(t1, t1 + \tau)$, and the exposure to the environmental contamination at time $t1$ resulting from the historical infectious number before $t1$. Our goal is to standardize the first part of the exposure in an observation time interval of unit length to an amount equal to the number of infectious individuals I_{t1}, which means $(\tau = 1)$ and $\frac{(-1+e^{-\mu}+\mu)}{\mu^2}\varphi I_{t1} = I_{t1}$. The shedding rate is then derived as $\varphi(\mu) = \frac{\mu^2}{-1+e^{-\mu}+\mu}$.

We plot $E(t)$ and the integral of $E(t)$ over time to illustrate the difference between scaling methods ($\varphi = 1$ and $\varphi(\mu) = \frac{\mu^2}{-1+e^{-\mu}+\mu}$). In an example scenario, one infectious individual is present for 1 day and removed after that. When the shedding rate is fixed at a constant (e.g. $\varphi = 1$ in the Fig. 3A & C), higher values of μ would lead to a lower $E(t)$ (Fig. 3A) and thus lower exposure to $E(t)$ (Fig. 3C). Eventually for $\mu \to \infty$, $E(t)$ is close to 0, plotted here by taking $\mu = 100$ per day (Green line in Fig. 3). With an observed infection probability during the first day, the transmission rate parameter increases with increasing μ because the exposure on the first day decreases with μ (Fig. 3C). However, when $(\mu) = \frac{\mu^2}{-1+e^{-\mu}+\mu}$, all the curves have the same exposure during the first day, i.e. equal to 1, for all the μ including $\mu \to \infty$ (red dot in Fig. 3D). When $\mu \to \infty$ (Green line in Fig. 3B), the exposure for each day is equal to 1 when $I_t = 1$ and 0 when $I_t = 0$, which is as expected for a direct transmission. The standardized exposure leads to a consistent interpretation of the transmission rate parameter.

The difference between more direct ($\mu = 100$) and more environmental transmission ($\mu = 0.01$) can be seen when we compare the infection probability on the second day (Fig. 3B). In more direct transmission, the infection probability on the second day would be zero as the exposure is zero (area under the green line in Fig. 3B on the second day). In contrast, the infection probability on the second day for environmental transmission would be non-zero, as the exposure is still present (area under the blue line in Fig. 3B on the second day). This straightforward interpretation is the advantage of our standardization that allows a consistent interpretation of transmission rate parameter among different μ.

This scaling method has the advantage of unifying the direct and environmental transmission. When $(\mu) = \frac{\mu^2}{-1+e^{-\mu}+\mu}$, $R = \frac{\beta\mu}{\alpha(-1+e^{-\mu}+\mu)}$The term $\frac{\mu}{(-1+e^{-\mu}+\mu)}$ can be interpreted as the total exposure to pathogens from the first day to infinity contributed by one infectious individual present one day $(1 + \frac{1-e^{-\mu}}{\mu} + \left(\frac{1-e^{-\mu}}{\mu}\right)^2 \ldots + \left(\frac{1-e^{-\mu}}{\mu}\right)^n + \ldots) = \frac{\mu}{(-1+e^{-\mu}+\mu)}$, where $\frac{1-e^{-\mu}}{\mu}$ is the fraction of exposure in the next day. The contribution of the first day's exposure when the infectious present is usually seen as the contribution of the direct transmission and the rest of exposure is usually seen as the indirect transmission via environment. Therefore, the reproduction ratio consists of two parts: the direct transmission ($\frac{\beta}{\alpha}$*1) when both susceptible and infectious individuals present at the same time, and the environmental transmission after infectious individuals being removed or recovered ($\frac{\beta}{\alpha}\frac{1-e^{-\mu}}{(-1+e^{-\mu}+\mu)}$). When $\mu \to \infty$, $(\frac{1-e^{-\mu}}{(-1+e^{-\mu}+\mu)}) \to 0$, hence the transmission is only contributed by direct transmission.

2.3. Stochastic simulation of environmental transmission model

As the exposure to environmental contamination has been derived in 1.2, we can now explain how to use such an environmental transmission model to simulate transmission. The two state transitions (infection or recovery) are modelled by a continuous-time discrete-state Markov

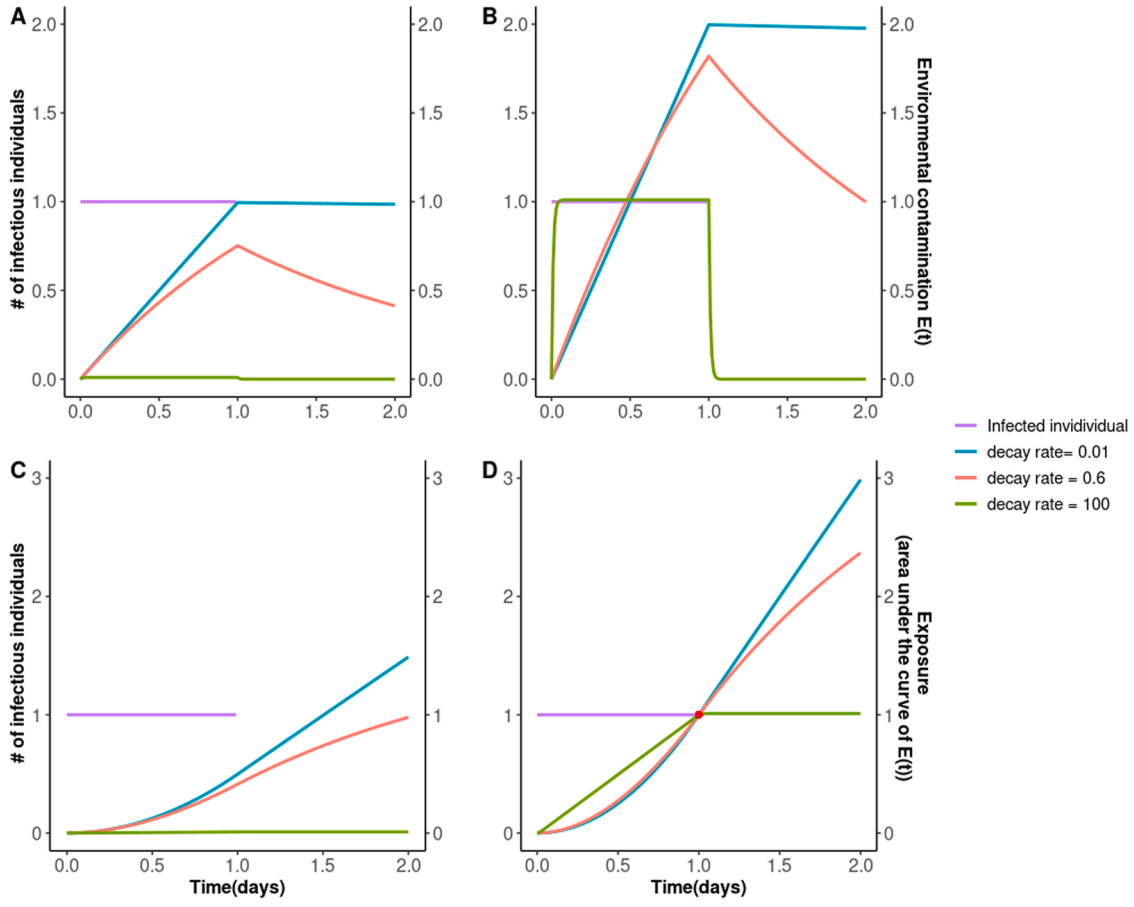

Fig. 3. The environmental contamination (at moment t) and the accumulated exposure (from 0 to t) to the environmental contamination, with two scaling methods for shedding rate. (A) & (B) show the changes of environmental contamination (at moment t) over time and (C) & (D) show the changes of accumulated exposure (from 0 to t) to environmental contamination over time. (A) & (C) represent the shedding rate $\varphi = 1$ and (B) & (D) represent the shedding rate $\varphi(\mu) = \frac{\mu^2}{-1+e^{-\mu}+\mu}$. The purple line shows that the infectious individual was present on the first day and removed on the second day. The blue, red and green lines show how the $E(t)$ changes over time, where the area under $E(t)$ represents the exposure. The red dot in the (D) shows that the exposure is unified to 1 among different decay rate parameter.

process via Gillespie's Direct Method (Gillespie, 1977). During an interval between two transition events $(t1, t2)$, S_t, I_t are constant equal to S_{t1} and I_{t1}, but the infection rate is not constant, due to the deterministic change in $E(t)$ given by Eq. (1). Therefore, we adjusted Gillespie's algorithm to consider the continuous changes in hazard rate with the corresponding rates summarised in Table 1.

The adjusted Gillespie's algorithm is as follow:

1. *Simulate the time that the next event occurs.*

a. *The probability of an event in an interval* $(t1, t1+\tau)$. The probability that one or more infection or recovery events occur during an interval follows a Poisson process, and the probability of no event occurring during τ is the zero term of the Poisson distribution with the expected number of events occurring during an interval τ as the parameter. Since, $E(t)$, in the instantaneous rate of getting infected (hazard rate$\beta\frac{S_{t1}E(t)}{N}$), is not a constant in the interval, the expected number of infections during $(t1, t1+\tau)$ depends on the area under the curve of $E(t)$, namely $\int_{t1}^{t1+\tau} E(t)dt$. Note, that when taking the integral over the environment one needs always to take into account the starting value $E(t)$ at the starting time $t1$.

$$P(no\,event in \tau) = e^{-\int_{t1}^{t1+\tau}(\beta\frac{S_{t1}}{N}E(t)-\alpha I_{t1})dt}$$

The hazard rate for a recovery is constant and thus its integral $\int_{t1}^{t1+\tau}\alpha I_{t1}dt$ is just the rate times τ i.e., $\alpha I_{t1}\tau$.

The probability that one or more events happens during an interval τ is $1 - P(no\ event\ in\tau)$.

b. Obtain a realisation of the random time interval between events through the inverse transform sampling technique. Random numbers are drawn from a uniform distribution $U(0,1)$ and the corresponding realisation of the random time interval τbetween events can be numerically determined by solving τ for each realisation of the random number p from distribution $U(0,1)$:

$$1\text{-}\ e^{-\beta\frac{S_{t1}}{N}\int_{t1}^{t1+\tau}E(t)dt-\alpha I_{t1}\tau} = p$$

2. *Simulate which event occurs*. The quotient of either the infection rate or the recovery rate over the interval τ over the sum of all rates in the interval determines which event happens at the time point determined by step 1. Given the value of τ as drawn by step 1, one of the events can be drawn from the probability of the events, for example, the probability of an infection event *given the interval* τ is:

$$\frac{\beta\frac{S_{t1}}{N}\int_{t1}^{t1+\tau}E(t)dt}{\beta\frac{S_{t1}}{N}\int_{t1}^{t1+\tau}E(t)dt+\alpha I_{t1}\tau}$$

Table 1
The processes in the interval $(t1, t1+\tau)$. Here the hazard rate for the interval is given, and the relation to the probability as explained in the text.

Process	Definition	The hazard rate for the event happening in interval $(t1, t1+\tau)$,
Infection	$(S_t, I_t) \rightarrow (S_t - 1, I_t + 1)$	$\int_{t1}^{t1+\tau}\beta\frac{S_{t1}E(t)}{N}dt = \beta\frac{S_{t1}}{N}\int_{t1}^{t1+\tau}E(t)dt$
Recovery	$(S_t, I_t) \rightarrow (S_t + 1, I_t - 1)$	$\int_{t1}^{t1+\tau}\alpha I_{t1}dt = \alpha I_{t1}\tau$

3. *Sampling procedure.* The simulated data are continuous in time while infection data are observed in discrete time intervals in reality. Here, we discretize the continuous-time to discrete-time because the observation of the infection data is on a discrete-time interval (e.g., on daily basis in this study). The number of infectious and susceptible individuals are observed at the beginning of each day. The number of new cases in each day is integrated over the discrete-time interval. The input parameters used in the baseline simulation scenario are listed below (Table 2).

Stochastic environmental transmission was simulated in 10 farms with 100 animals for each farm, starting with a clean environment and 10 infectious animals in each farm or from a pseudo-endemic state with 67 infectious animals in each farm with the equilibrium environmental infectious pressure ($\frac{\mu}{-1+e^{-\mu}+\mu}$*67 = 2720 units for μ = 0.05 per day). The simulation results for transmission in the baseline scenario (using parameters in Table 2) including a transient phase and a pseudo-endemic phase were shown Fig. 4.

2.4. Comparing estimation methods

The simulated infection data were used to assess two different estimation methods, exposure-based and trajectory-based, in back-estimating the underlying parameters μ and β. The recovery rate parameter can be estimated when individual level data on infection status is available; therefore, the parameter can be assumed to be known in the comparison below. The shedding rate parameter is also not estimated because it is a function of decay rate parameter. The analysis was done separately for the transient phase (Fig. 4A) and the pseudo-endemic phase (Fig. 4B).

2.4.1. Exposure-based estimation method

We fitted the stochastic transmission model to exposure data using maximum likelihood estimation. The exposure was calculated from observed infection data and the past number of infectious individuals was considered in the calculation. In particular, the number of new cases over each observation time interval $(i, i+1)$, follows a binomial distribution with probability $1-e^{\frac{-\beta(\int_i^{i+1}E(t|I_i,E(i))dt)}{N}}$ and binomial total S_i, the number of susceptible individuals at i time where $i, i+1$ are the discrete integer time intervals. The likelihood as a function of $\beta and \mu$ is given by

$$\mathscr{L}(\theta) = \prod_i (1-e^{\frac{-\beta(\int_i^{i+1}E(t|I_i,E(i))dt)}{N}})^{cases_i}\ (e^{\frac{-\beta(\int_i^{i+1}E(t|I_i,E(i))dt)}{N}})^{(S_i-cases_i)}$$

where $cases_i$ is the observed number of new cases (obtained by summation in the simulation) in the interval $(i, i+1)$. The challenge in this likelihood function is that is μ is inside $\int_i^{i+1}E(t|I_i,E(i))dt$ which needs to be constructed by iterating Eqs. (2) and (3).

To profile the likelihood of μ, a set of μ is used to construct the time-series exposure dataset for each day $(\int_i^{i+1}E(t|I_i,E(i))dt)$. Then for each exposure dataset, $\log(\mathscr{L}(\beta))$ is maximized. The optimization can be

Table 2
Input values for the environmental transmission simulation.

Variables	Definition	Value
β	Environmental transmission rate parameter	0.0015 (day^{-1})
α	Recovery rate parameter	0.02 (day^{-1})
μ	Decay rate parameter	0.05 (day^{-1})
φ	Shedding rate parameter	$\frac{\mu^2}{-1+e^{-\mu}+\mu} = 2.02$ (day^{-1})

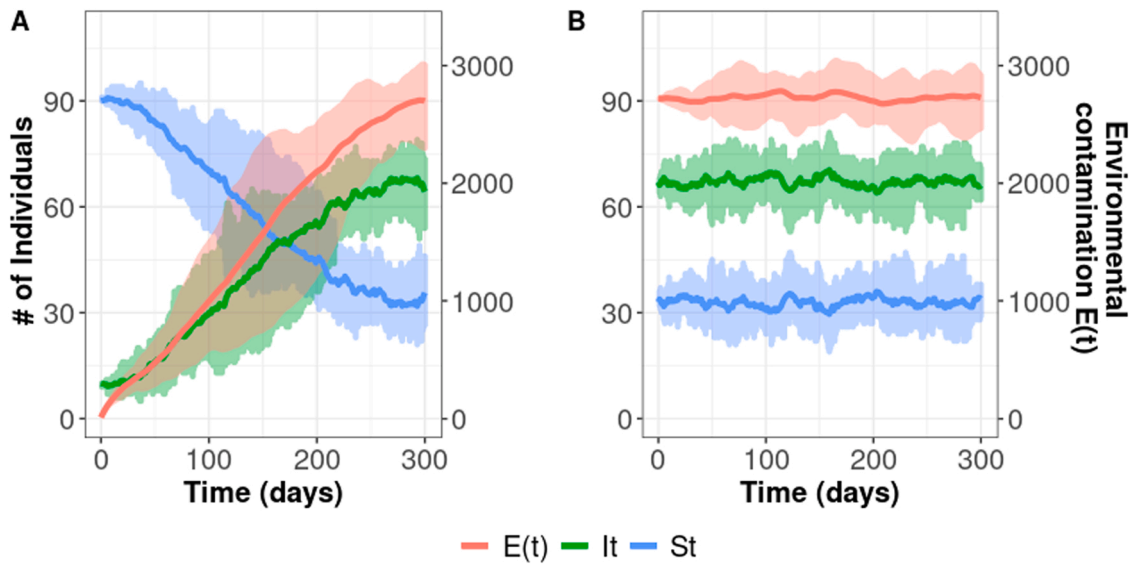

Fig. 4. The simulation results for the transmission in a transient phase (A) and in a pseudo-endemic phase (B). The red lines represent the number of infectious individuals I_t, blue lines the number of susceptible individuals S_t and green lines the environmental contamination $E(t)$. Coloured areas show the envelop from 10 simulation repeats and solid lines show the average of simulations.

achieved by defining a generalized linear model with cloglog link since the expected number of cases in each day follows: $\mathbb{E}(cases_i) = S_i(1 - e^{-\frac{\beta(\int_i^{i+1} E(t|I_i,E(i))dt)}{N}})$. Transforming the formula with the cloglog link, we derive:

$$\log\left(-\log\left(1-\mathbb{E}(\frac{cases_i}{S_i})\right)\right) = \log(\beta) + \log\left(\frac{\int_i^{i+1} E(t|I_i,E(i))dt}{N}\right), \quad (4)$$

where $\log(\beta)$ is the intercept and $\log\left(\frac{\int_i^{i+1} E(t|I_i,E(i))dt}{N}\right)$ is an offset, which is an explanatory variable with the coefficient equal to 1 and which depends on the historical infection data and decay rate parameter μ. The estimated β can be calculated as $\widehat{\beta} = e^{C0}$, where C_0 is the estimated intercept from Eq. (4). The AIC value for each μ constructed exposure dataset is calculated by $-2*\log(\mathscr{L}(\beta))+4$ and plotted against the μ (Fig. 5A & D). In addition, we maximized the $\log(\mathscr{L}(\mu))$ for a set of β and thus obtained the profile likelihood for β (Fig. 5B & E). To obtain a profile likelihood of R, a grid of β and μ were generated and the AIC of each pair of β and μ is calculated. Then for each R, the minimum AIC value is plotted against R (Fig. 5C & F). The likelihood surface is visualized by a 2D contour plot (Fig. 7).

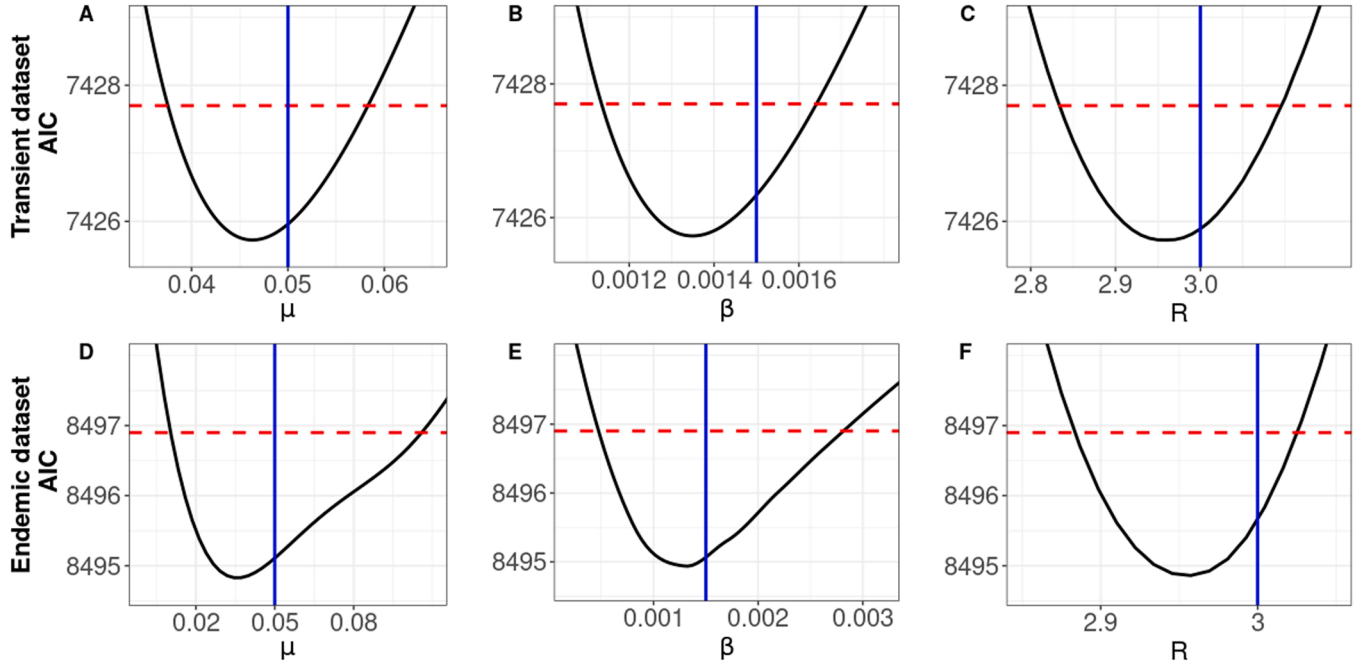

Fig. 5. Profile likelihood for parameters by exposure-based estimation. The first row (A–C) analysed transient phase and the second row (D–F) analysed the pseudo-endemic phase. In the different columns the profile likelihood of β, μ and R are shown respectively. The blue solid lines represent the input parameter values and the intercepts of red dashed lines and black lines represent confidence bounds of the estimation by showing minimum AIC value plus 2.

2.4.2. Trajectory-based estimation method

Trajectory-based method, also called trajectory matching or curve fitting, is used frequently to estimate parameters for dynamic systems. This method conducts the inference with a deterministic model assuming that the dynamic process is deterministic, and the observation error is the only cause of variation between trajectory modelled and the observed data. The ODE model with environmental transmission can be simulated as follows.

$$\frac{dS}{dt} = -\beta\frac{ES}{N} + \alpha I$$

$$\frac{dI}{dt} = \beta\frac{ES}{N} - \alpha I$$

$$\frac{dE}{dt} = \varphi I - \mu E$$

To fit the deterministic trajectory to infection data, one needs to include stochasticity into the model by adding a random error to the trajectory values. The maximum likelihood method returns the log-likelihood of the data, given some combination of parameters and then via optimizing algorithms it gives parameter pairs with the maximum likelihood. The observation errors can also be assumed to follow other distributions than Gaussian, such as Binomial, or Poisson. We used the POMP package using maximum likelihood estimation assuming Gaussian distribution (King et al., 2015) because it is the most commonly assumed distribution and most distributions generate a similar fit to data (Eisenberg et al., 2013; Goeyvaerts et al., 2015). A Nelder-Mead search was used to optimize parameters. The likelihood function can be written as:

$$\mathscr{L}(\theta) = \prod_i \frac{1}{\sqrt{2\pi\sigma^2}} e^{\left(-\frac{(I_i - Y_i)^2}{2\sigma^2}\right)}$$

where I_i is the observed number of infectious at each time interval and Y_i is the solution of ODE models and σ is the variance for measurement. To profile over a parameter, we fix the value of that parameter at each of several values, then maximize the likelihood over the remaining parameter (Fig. 6). The likelihood surface is visualized by a 2D contour plot.

2.4.3. Estimation results

Using the exposure-based estimation method, we obtained accurate estimates for the transmission rate parameter (β), decay rate parameter (μ) and the basic reproduction ratio (R). The input values (blue lines in Fig. 5) fall inside the confidence bounds, which is where the red dashed lines (minimum AIC + 2) cross the profile likelihood, for both transient and pseudo- endemic phases. This can also be seen in the likelihood contour plot, where input parameters are well inside the contour plots (Fig. 7A & B). The pseudo-endemic phase yielded wider confidence bounds for both β and μ, compared to the transient phase.

In comparison, the trajectory-based method performed worse in back-estimation of the parameters. While β and μ estimated by trajectory-based method are still close to the input values in the transient phase dataset, the input values are actually outside the confidence bounds (Fig. 6 A–C). The confidence bounds and the likelihood contour (Fig. 7C) are both very narrow from the transient phase dataset. For the pseudo-endemic phase dataset, both $\widehat{\mu}$ and $\widehat{\beta}$ have wide confidence bounds (Fig. 6 D, E) with an open contour plot (Fig. 7D) and hence parameters cannot be estimated back. Even though the reproduction ratio can be estimated, wrong estimates for $\widehat{\mu}$ and $\widehat{\beta}$ can form misleading information on the relative importance of direct and environmental transmission in a system.

2.4.4. The comparison of two statistical methods

As we found that the exposure-based estimation performed better than the trajectory-based estimation (Figs. 5 and 6), we investigated the reason by calculating the autocorrelation for the residuals from the two statistical models (Fig. 8). To estimate the transmission parameters back, statistical models need to use the autocorrelation information in infection data, because the transmission process is about the correlation in time between infectious individuals in the past and infections occurring later on. Therefore, residuals for a correctly fitting model should have no autocorrelation, because the statistical model should capture all the autocorrelation. We found that the residuals from the exposure-based

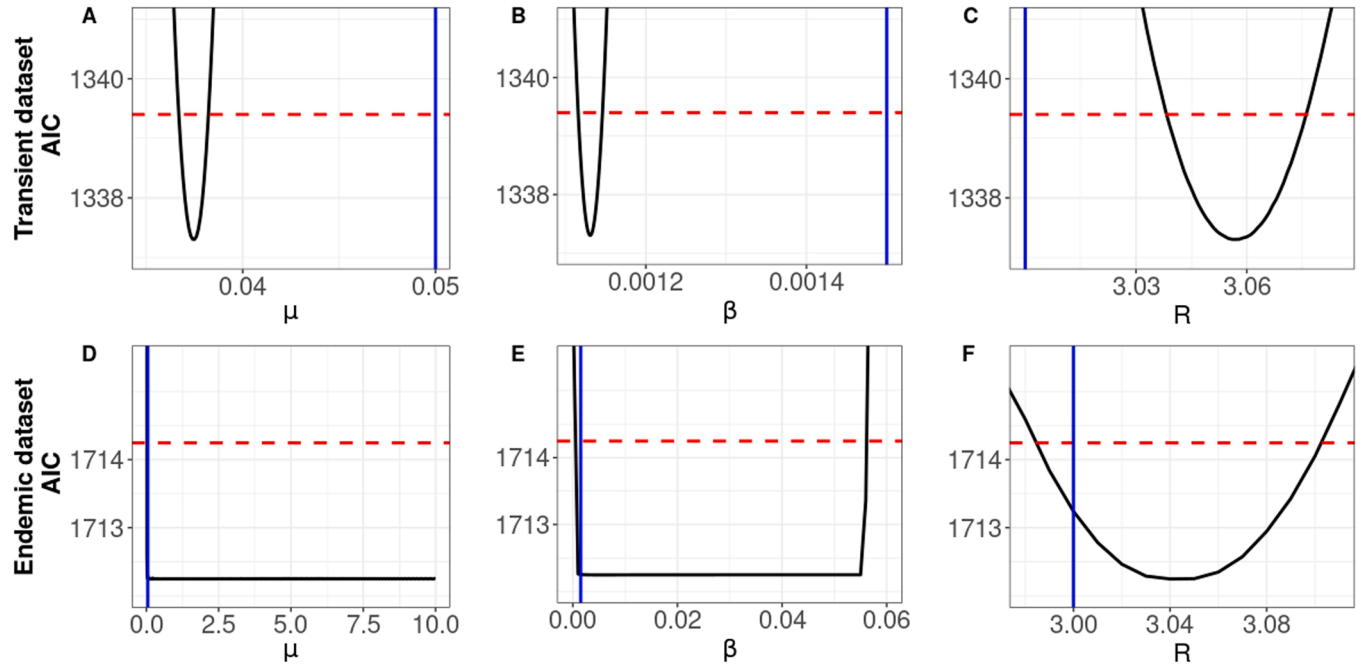

Fig. 6. Profile likelihood for parameters by trajectory-based estimation. The first row (A–C) analysed transient phase and the second row (D–F) analysed the pseudo-endemic phase. In the different columns the profile likelihood of β, μ and R are shown respectively. The blue solid lines represent the input parameter values and the intercepts of red dashed lines and black lines represent confidence bounds of the estimation by showing minimum AIC value plus 2.

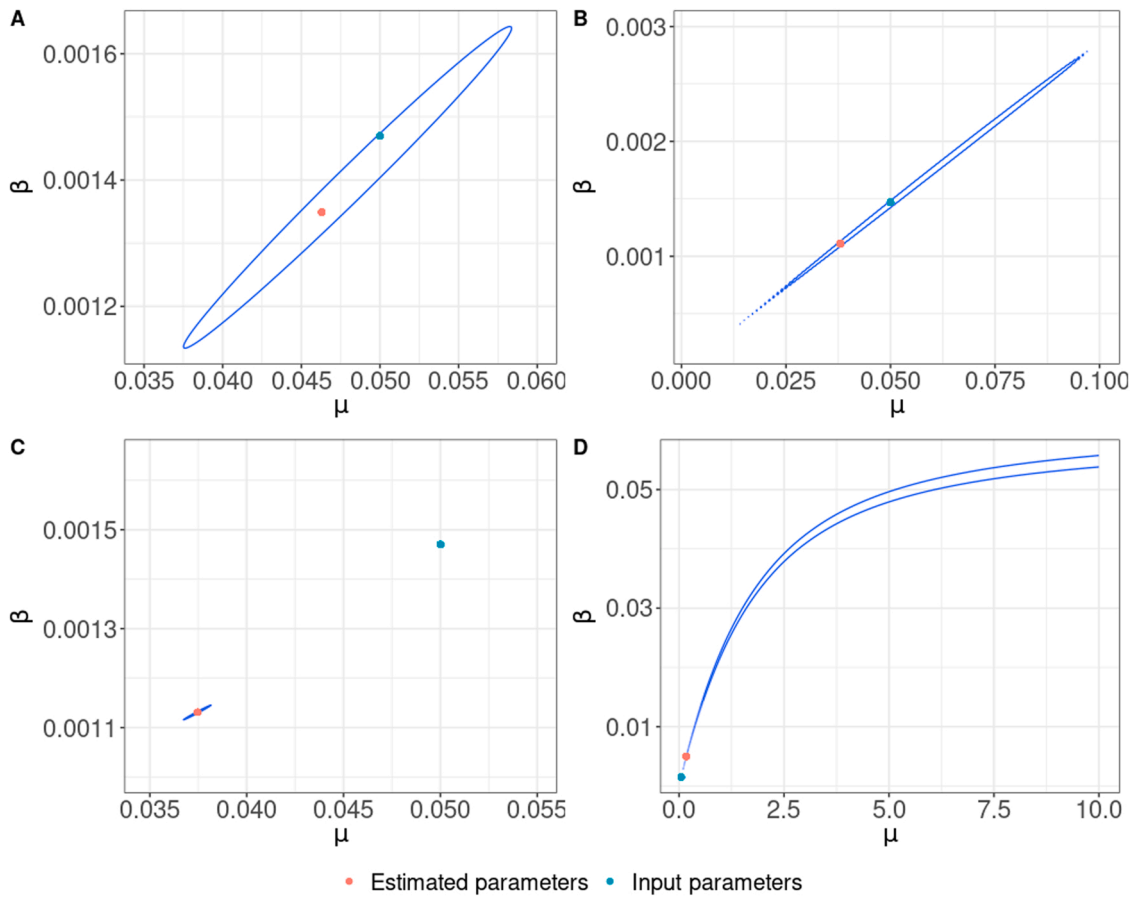

Fig. 7. The 2D contour plots where the blue line ellipses show confidence bounds (minimum AIC value plus 2). (A) shows the contour plot for the exposure-based method with the transient phase and (B) with the pseudo-endemic phase. (C) and (D) show the contour plot for the trajectory-based method with the transient phase and the pseudo-endemic phase. The red dots show the estimated values for β and μ and the blue dots represent the input values for β and μ.

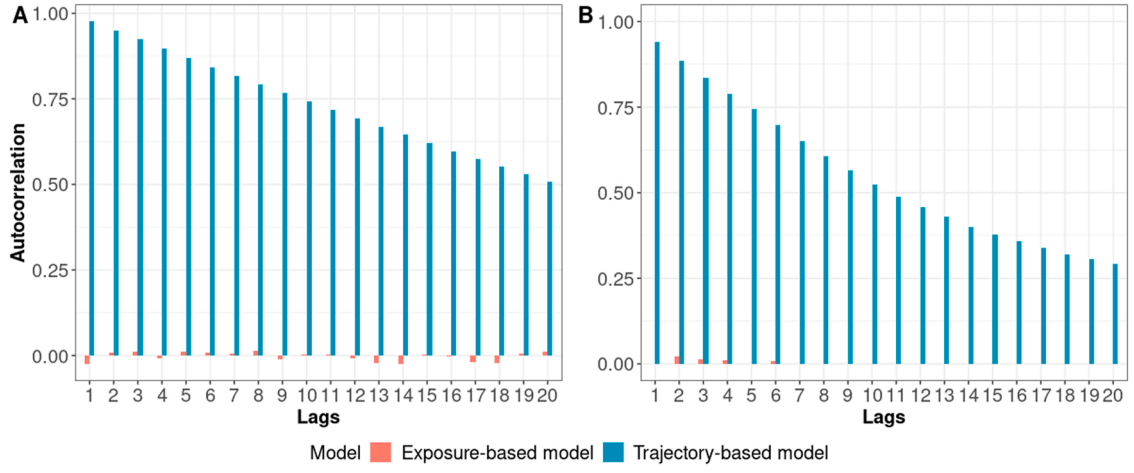

Fig. 8. The autocorrelation of residuals. Red bars represent the autocorrelation of residuals from the exposure-based statistical model and blue bars from the trajectory-based statistical model. (A) shows the autocorrelation in the transient phase and (B) in the pseudo-endemic phase.

method have no significant autocorrelation; this is the case for the transient as well as the pseudo-endemic phase (red bars in Fig. 8). However, the residuals from the trajectory-based method show high autocorrelation, which indicates that a large part of the autocorrelation information in the infection data is not captured by the trajectory-based method.

The exposure-based estimation method links the probability of infection to exposure using a dose-response equation, where the exposure is calculated from the observed historical number of infectious individuals. In this way, each observed datapoint can change the prediction of exposure-based estimation model in the future. The more recent observed data matter more for what happens in the next observation time step in the exposure-based method, leading to a higher autocorrelation in the infection data at smaller time lags. Therefore, the exposure-based method does use the autocorrelation information in the infection data and leaves no autocorrelation in residuals. In comparison,

in the trajectory-based method, the trajectories are determined by varying the set of parameters and the possible initial infection data and then the best fit trajectory is selected by comparing these different trajectories with observed data. Selecting best fit trajectory is only influenced by observed data in a way that it accounts for the uncertainty in observing each datapoint by using the correlations with all past and all future observations. The trajectory-based estimation method, therefore, cannot fully use the autocorrelation information in the data and thus autocorrelation remains present in the residuals.

2.5. Sensitivity analysis on transmission quantification

Sensitivity analysis was performed to test whether exposure-based estimation can estimate back β, μ and R under scenarios with different input parameters in data simulation. There are three independent input parameters (α, μ and β) during simulation. The recovery rate parameter (α) is assumed to be known and not involved in parameter estimation nor sensitivity analysis. The decay rate parameter (μ) is a relative value to the observation time unit. When the observation interval is too big compared to the value of the decay rate parameter, the pathogen dynamics occur fast and infection dynamics behave similarly to direct transmission (Breban, 2013). Although the fast decay rate parameters could hamper the practical joint identifiability of β and μ (see sensitivity analysis of μ in Supplement Fig. S1), this practical identifiability can be improved by increasing the observation intervals.

Therefore, here we present whether changing input transmission rate parameter β would influence the estimation of β, μ and R. For each β, the other two input parameters α, μ were fixed at the values shown in Table 2. A dataset including the transient phase and the pseudo-endemic phase were simulated with 10 repeats for each dataset. The input values (red lines) fell within confidence bounds of estimation (Fig. 9). This means that the estimation of β, μ and R is not sensitive to the choice of input β in both transient phase and pseudo-endemic phase datasets. The exposure-based estimation method is robust for environmental transmission.

The sensitivity analysis for the trajectory-based method showed that estimates were not correct and different input parameters did not improve parameter estimations (see Supplement S3).

2.6. Application: impact of disinfection and estimation of minimum disinfection frequency

An important aim of correctly estimating parameters is to correctly predict the effect of interventions by extrapolating models. We will now show an application of our approach, by quantifying the impact of an often-used control measure: routine disinfection. This intervention is one of the most important and standard preventive measures for all infectious diseases, but especially for diseases for which few other interventions are available e.g., norovirus in humans, African Swine fever in pigs, and antimicrobial resistant microorganisms in animals and hospitals. We derive the impact of routine disinfection on the reduction of R_0, using the environmental modelling approach presented in this paper. This analysis is done to illustrate that correctly estimated parameters are crucial for drawing correct conclusions on whether interventions targeted at the environment are sufficient to control an infectious disease.

When introducing routine disinfection with a frequency once every x days, the original equilibrium breaks, and the number of infectious individuals decreases as the environmental contamination is reduced. The transmission dynamics gradually reach a new equilibrium where the total number of infectious individuals in x days is again the same as the number of recovered individuals. The environmental contamination $E(t)$ changes periodically from 0 after disinfection to a certain level until the next disinfection. The total exposure to the environmental contamination during this x days can be derived from Eq. (3) as $\frac{-1+e^{-\mu x}+\mu x}{-1+e^{-\mu}+\mu} I_t$. In the equilibrium stage, the total number of infections in an interval between two disinfection is therefore $\beta \frac{-1+e^{-\mu x}+\mu x}{-1+e^{-\mu}+\mu} I^* \frac{S^*}{N}$, where I^*, S^* represent the number of infectious and susceptible individuals at the equilibrium. The total number of recovered individuals during the interval x is $\alpha I^* x$, which equals the number of new cases, leading to: $\beta \frac{-1+e^{-\mu x}+\mu x}{-1+e^{-\mu}+\mu} I^* \frac{S^*}{N} = \alpha I^* x$. Hence, we derive the effective reproduction ratio for after disinfection:

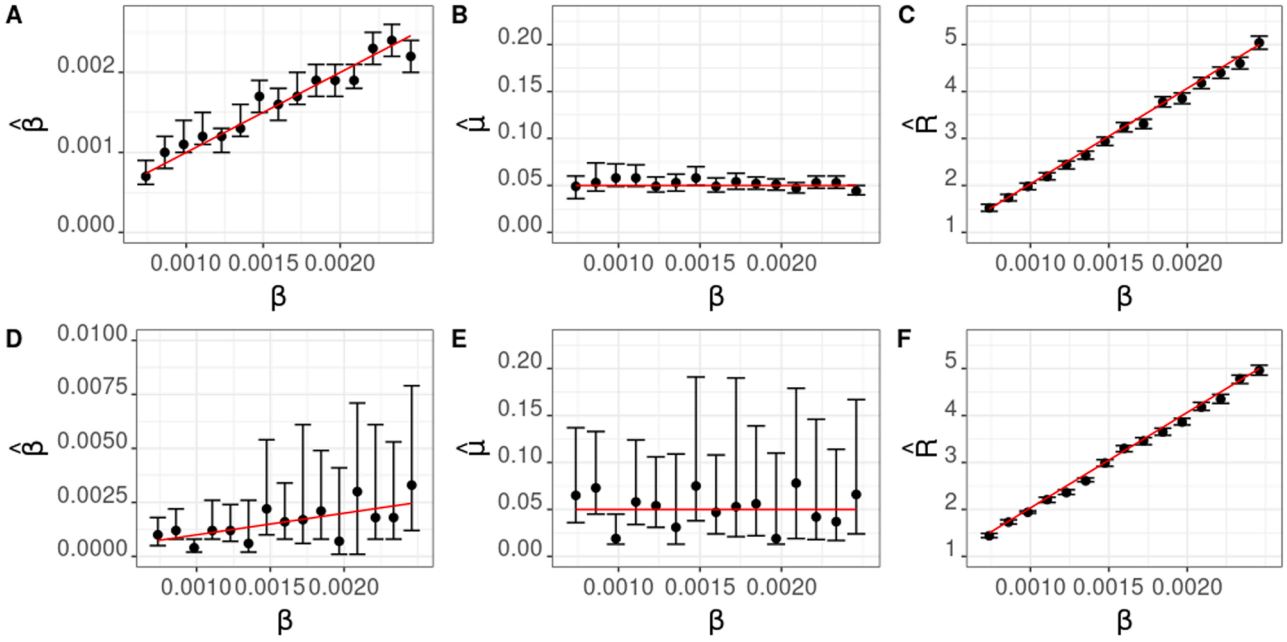

Fig. 9. The sensitivity analysis on the impact of different input β on parameters estimation ($\hat{\beta}$, $\hat{\mu}$ and $\hat{R}$) by the exposure-based method. The first row (A–C) analysed transmissions from a transient phase while the second row (D–F) analysed transmission from a pseudo-endemic phase. (A, D) show parameter estimation forβ, (B, E) for μ and (C, F) for R among different datasets. The red solid lines represent the true parameter values. The dots represent the estimated parameters with the error bar.

$$R_{disinfection} = \frac{N}{S^*} = \frac{-1 + e^{-\mu x} + \mu x}{(-1 + e^{-\mu} + \mu)x} \frac{\beta}{\alpha}$$

where $R_{disinfection}$ represents the effective reproduction ratio under a regime of disinfection. With estimates of decay rate and transmission rate parameters, one can predict the minimum regular disinfection frequency (Supplement S4).

We use an example to show how important the correct estimation of decay rate and transmission rate parameters is regarding predicting interventions. The example infection has a basic reproduction ratio $R = 3$ with the decay rate 0.1 per day (the lowest pink line in Fig. 10). In this infection, the disinfection impact is very effective, as a disinfection routine every 8 days would be sufficient to control this infection by bringing the R below 1. However, with the wrong estimation of decay rate and transmission rate parameters given the correct estimation of R, the interpretation of disinfection impact can be very incorrect and misleading. For example, if the decay rate is estimated as 3 per day (the highest line in Fig. 10), the disinfection routine every 8 days would not be sufficient because it only has a marginal reduction on R ($R_{disinfection} = 2.7$). Even with a daily disinfection routine, the $R_{disinfection}$ is still above 1, which leads to the wrong conclusion that disinfection is not effective and is not able to control this infection. Therefore, only with the right estimation of decay rate parameter and transmission rate parameter can we predict interventions correctly.

3. Discussion

A better understanding of environmental transmission is of vital importance for assessing and predicting the impact of intervention measures. Although risk factor analysis has been widely used to assess the impact of interventions (Aiello et al., 2008; Cairncross et al., 2010; Liang et al., 2020), it has limitations in predicting future risks or risks under different scenarios. Hence, dynamic models have often been preferred (Woolhouse, 2011). However, dynamic models for environmental transmission have difficulties in jointly identify underlying parameters. Therefore, this paper aims to improve the estimation for environmental transmission models by introducing a novel scaling method and using calculated exposure for a better understanding of environmental transmission and prediction of environmental interventions.

Our novel scaling method uses a continuous decay rate parameter to distinguish more direct from more environmental transmission. A continuous decay rate aligns with the reality that direct and environmental transmission lie along a continuum. Direct transmission can be seen as a special case of environmental transmission where pathogens have an extremely high decay rate in the environment (Cortez, 2021; Cortez and Duffy, 2021; Cortez and Weitz, 2013; Eisenberg et al., 2013; Espira et al., 2022). For example, droplets transmission, often seen as direct transmission, can be modelled as environmental transmission with pathogens decaying in a few minutes (Duives et al., 2021) In addition to the unification of direct and environmental transmission models, transmission model with this scaling method still provides the relative contribution of the environment and the direct contact to the transmission.

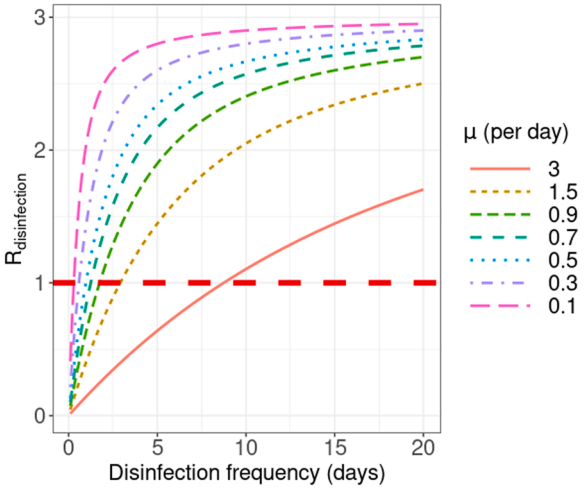

Fig. 10. The effective reproduction ratio after disinfection($R_{disinfection}$) under different disinfection frequencies. The different colour lines showed transmissions with different decay rate, but all the transmissions have the same basic reproduction ratio ($R = 3$). The intercept of $R_{disinfection}$ with the red dashed line (R = 1) represents the minimum required disinfection frequency to bring R below 1.

In comparison, other studies usually assume two transmission routes when the environment is involved (Eisenberg et al., 2013; Towers et al., 2018). One route accounts for the transmission when susceptible and infectious individuals are present at the same time, and another route accounts for environmental transmission routes (or so-called indirect routes) (Dekker et al., 2020; Eisenberg et al., 2013; Towers et al., 2018). However, with only infection data, the estimations might not represent the true mechanisms and reproduction ratio R (Lee et al., 2017). This can be understood intuitively by an example: an animal getting infected directly by licking another infectious animal cannot be distinguished from licking excreta that have been shed very recently by infectious animals (Almberg et al., 2011). Therefore, our method of unifying the undistinguishable two routes provides a good alternative to understanding the transmission mechanism.

We show that our exposure-based estimation can jointly estimate transmission rate and decay rate parameters. In comparison, the commonly used trajectory-based estimation method failed to correctly identify the parameter values, as the true parameters often fell outside the confidence bounds. This confirms the findings of Lee et al. (2017) which also showed that this trajectory-based model cannot estimate back the transmission parameters and R. However, our study is the first to solve this issue by using a novel exposure-based estimation method in environmental transmission. In addition, our sensitivity analysis also showed the robustness of the exposure-based estimation and the limitation that observations need to be frequent enough relative to the decay rate parameter (Supplement S2).

The exposure-based method performs better because it makes use of autocorrelation by giving the correct weight to data from previous observation periods. One may argue that our infection data are simulated with autocorrelation which is not a compulsory choice. The choice to model the transmission process in this way is based on the notion that the transmission process in real life is all about the correlation in time and space, due to the nature of the spread of infections and infectious particles in time and space. The number of new cases is assumed to depend on the actual number of infectious individuals in the previous time points through environments, which has been used in many stochastic simulation models (Nixon et al., 2021; Widgren, Bauer, et al., 2016; Widgren, Engblom, et al., 2016).

This model assumes the independent action of each pathogen which means each pathogen has the same probability of infecting other individuals. The underlying dose-response function is the exponential function, as can be seen for example from the likelihood formula (6), while other dose-response functions such as linear, exact-Poisson, approximate beta-Poisson, and log-normal functions can be assumed but were not studied in this paper (Brouwer et al., 2017). The transmission rate, decay rate and shedding rate parameters are assumed as constant in this model, while this is unlikely to hold for many environmentally transmitted pathogens (Chin et al., 2020). Future research is needed for example for the parameterization of the nonconstant decay rate.

Furthermore, we show how transmission models with correct parameter estimation can be extrapolated to predict interventions correctly. To illustrate this, we derived the formula to predict the

maximum disinfection impact on reducing the reproduction ratio. This prediction can provide important suggestions on infection control. For example, for pathogens with a high decay parameter in the environment, the disinfection alone may not be able to bring the $R_{disinfection}$ below 1 regardless of high disinfection frequency. Thus, other interventions that target removing the infectious individuals from the environment such as quarantine or culling infectious animals are needed. On the other hand, for pathogens with a low decay parameter in the environment, the interventions such as test and removal, quarantine may not be able to bring R below one 1 and disinfection and environmental interventions that remove pathogens in the environment are of crucial. Only with the correct estimation of transmission rate and decay rate parameters, can we predict interventions correctly and select effective control measures.

CRediT authorship contribution statement

You Chang: Conceptualization, Methodology, Data analysis, Visualization, Writing – original draft, Writing – review & editing. **Mart de Jong:** Conceptualization, Investigation, Writing – original draft, Writing – review & editing, Supervision, Funding acquisition.

Funding

This work was supported by the Irish Department of Agriculture, Food and the Marine's Research Funding Programme as part of the project "Two host species transmission data analysis and modelling to calculate the risk maps for bovine Tb during eradication by badger vaccination in Ireland".

Declaration of Competing Interest

The authors declare that they have no known competing financial interests or personal relationships that could have appeared to influence the work reported in this paper.

Acknowledgment

We thank Nienke Hartemink for her very helpful discussion and suggestions, which led to considerable improvements of the manuscript.

Appendix A. Supporting information

Supplementary data associated with this article can be found in the online version at doi:10.1016/j.epidem.2023.100672.

References

Aiello, A.E., Coulborn, R.M., Perez, V., Larson, E.L., 2008. Effect of hand hygiene on infectious disease risk in the community setting: a meta-analysis. Am. J. Public Health 98 (8), 1372–1381. https://doi.org/10.2105/AJPH.2007.124610.

Allen, A.R., Ford, T., Skuce, R.A., 2021. Does Mycobacterium tuberculosis var. bovis survival in the environment confound bovine tuberculosis control and eradication? A literature review. Vet. Med. Int. 2021. https://doi.org/10.1155/2021/8812898.

Almberg, E.S., Cross, P.C., Johnson, C.J., Heisey, D.M., Richards, B.J., 2011. Modeling routes of chronic wasting disease transmission: environmental prion persistence promotes deer population decline and extinction. PLoS One 6 (5), e19896. https://doi.org/10.1371/journal.pone.0019896.

Ashbolt, N.J., 2004. Microbial contamination of drinking water and disease outcomes in developing regions. Toxicology 198 (1–3), 229–238. https://doi.org/10.1016/j.tox.2004.01.030.

Biemans, F., Bijma, P., Boots, N.M., de Jong, M.C.M., 2018. Digital dermatitis in dairy cattle: the contribution of different disease classes to transmission. Epidemics 23, 76–84. https://doi.org/10.1016/j.epidem.2017.12.007.

Bijma, P., Hulst, A.D., de Jong, M.C.M., 2022. The quantitative genetics of the prevalence of infectious diseases: hidden genetic variation due to indirect genetic effects dominates heritable variation and response to selection [Article]. Genetics 220 (1), iyab141. https://doi.org/10.1093/genetics/iyab141.

Bootsma, M.C., Bonten, M.J., Nijssen, S., Fluit, A.C., Diekmann, O., 2007. An algorithm to estimate the importance of bacterial acquisition routes in hospital settings. Am. J. Epidemiol. 166 (7), 841–851. https://doi.org/10.1093/aje/kwm149.

Bouwknegt, M., Frankena, K., Rutjes, S.A., Wellenberg, G.J., de Roda Husman, A.M., van der Poel, W.H., de Jong, M.C., 2008. Estimation of hepatitis E virus transmission among pigs due to contact-exposure. Vet. Res. 39 (5), 1.

Breban, R., 2013. Role of environmental persistence in pathogen transmission: a mathematical modeling approach. J. Math. Biol. 66 (3), 535–546. https://doi.org/10.1007/s00285-012-0520-2.

Brouwer, A.F., Eisenberg, M.C., Love, N.G., Eisenberg, J.N., 2018. Persistence-infectivity trade-offs in environmentally transmitted pathogens change population-level disease dynamics. arXiv Prepr. arXiv (1802.05653).

Brouwer, A.F., Weir, M.H., Eisenberg, M.C., Meza, R., Eisenberg, J.N.S., 2017. Dose-response relationships for environmentally mediated infectious disease transmission models. PLoS Comput. Biol. 13 (4), e1005481 https://doi.org/10.1371/journal.pcbi.1005481.

Cairncross, S., Hunt, C., Boisson, S., Bostoen, K., Curtis, V., Fung, I.C., Schmidt, W.P., 2010. Water, sanitation and hygiene for the prevention of diarrhoea [Article]. Int. J. Epidemiol. 39 (SUPPL. 1), Si193–Si205. https://doi.org/10.1093/ije/dyq035.

Chen, S., Sanderson, M.W., White, B.J., Amrine, D.E., Lanzas, C., 2013. Temporal-spatial heterogeneity in animal-environment contact: implications for the exposure and transmission of pathogens. Sci. Rep. 3 (1), 3112. https://doi.org/10.1038/srep03112.

Chin, A.W.H., Chu, J.T.S., Perera, M.R.A., Hui, K.P.Y., Yen, H.-L., Chan, M.C.W., Peiris, M., Poon, L.L.M., 2020. Stability of SARS-CoV-2 in different environmental conditions. Lancet Microbe 1 (1). https://doi.org/10.1016/s2666-5247(20)30003-3.

Cortez, M.H., 2021. Using sensitivity analysis to identify factors promoting higher versus lower infection prevalence in multi-host communities. J. Theor. Biol. 526, 110766 https://doi.org/10.1016/j.jtbi.2021.110766.

Cortez, M.H., Duffy, M.A., 2021. The context-dependent effects of host competence, competition, and pathogen transmission mode on disease prevalence. Am. Nat. 198 (2), 179–194. https://doi.org/10.1086/715110.

Cortez, M.H., Weitz, J.S., 2013. Distinguishing between indirect and direct modes of transmission using epidemiological time series. Am. Nat. 181 (2), E43–E52. https://doi.org/10.1086/668826.

Corbett, C.S., de Jong, M., Orsel, K., De Buck, J., Barkema, H.W., 2019. Quantifying transmission of Mycobacterium avium subsp. paratuberculosis among group-housed dairy calves. Vet. Res. 50 (1), 1–14. https://doi.org/10.1186/s13567-019-0678-3.

De Jong, M.C.M., 1995. Mathematical modelling in veterinary epidemiology: why model building is important. Prev. Vet. Med. 25 (2), 183–193. https://doi.org/10.1016/0167-5877(95)00538-2.

de Rueda, C.B., de Jong, M.C., Eblé, P.L., Dekker, A., 2015. Quantification of transmission of foot-and-mouth disease virus caused by an environment contaminated with secretions and excretions from infected calves. Vet. Res. 46 (1), 1–12. https://doi.org/10.1186/s13567-015-0156-5.

Dekker, A., van Roermund, H.J., Hagenaars, T.J., Eblé, P.L., de Jong, M.C., 2020. Mathematical quantification of transmission in experiments: FMDV transmission in pigs can be blocked by vaccination and separation. Front. Vet. Sci. 7. https://doi.org/10.3389/fvets.2020.540433.

Diekmann, O., Heesterbeek, J.A., Roberts, M.G., 2010. The construction of next-generation matrices for compartmental epidemic models. J. R. Soc. Interface 7 (47), 873–885. https://doi.org/10.1098/rsif.2009.0386.

Duives, D., Chang, Y., Sparnaaij, M., Wouda, B., Boschma, D., Liu, Y., Yuan, Y., Daamen, W., de Jong, M.C.M., Teberg, C., Schachtschneider, K., Sikkema, R., van Veen, L., ten Bosch, Q., 2021. The multi-dimensional challenges of controlling SARS-CoV-2 transmission in indoor spaces: insights from the linkage of a microscopic pedestrian simulation and virus transmission models. medRxiv. https://doi.org/10.1101/2021.04.12.21255349.

Eblé, P., Hagenaars, T., Weesendorp, E., Quak, S., Moonen-Leusen, H., Loeffen, W., 2019. Transmission of African Swine Fever Virus via carrier (survivor) pigs does occur. Vet. Microbiol. 237, 108345. ⟨https://www.sciencedirect.com/science/article/pii/S0378113519302457?via%3Dihub⟩.

Eisenberg, M.C., Robertson, S.L., Tien, J.H., 2013. Identifiability and estimation of multiple transmission pathways in cholera and waterborne disease. J. Theor. Biol. 324, 84–102. https://doi.org/10.1016/j.jtbi.2012.12.021.

Erazo, D., Pedersen, A.B., Gallagher, K., Fenton, A., 2021. Who acquires infection from whom? Estimating herpesvirus transmission rates between wild rodent host groups. Epidemics 35, 100451. ⟨https://www.sciencedirect.com/science/article/pii/S175543652100013X?via%3Dihub⟩.

Espira, L.M., Brouwer, A.F., Han, B.A., Foufopoulos, J., Eisenberg, J.N.S., 2022. Dilution of epidemic potential of environmentally transmitted infectious diseases for species with partially overlapping habitats. Am. Nat. 199 (2), E43–E56. https://doi.org/10.1086/717413.

Gillespie, D.T., 1977. Exact stochastic simulation of coupled chemical reactions. J. Phys. Chem. 81 (25), 2340–2361.

Goeyvaerts, N., Willem, L., Van Kerckhove, K., Vandendijck, Y., Hanquet, G., Beutels, P., Hens, N., 2015. Estimating dynamic transmission model parameters for seasonal influenza by fitting to age and season-specific influenza-like illness incidence. Epidemics 13, 1–9. https://doi.org/10.1016/j.epidem.2015.04.002.

Grassly, N.C., Fraser, C., 2008. Mathematical models of infectious disease transmission. Nat. Rev. Microbiol. 6 (6), 477–487. https://doi.org/10.1038/nrmicro1845.

Halloran, M.E., Longini Jr, I.M., Struchiner, C.J., 1999. Design and interpretation of vaccine field studies [Review]. Epidemiol. Rev. 21 (1), 73–88. https://doi.org/10.1093/oxfordjournals.epirev.a017990.

Kermack, W.O., McKendrick, A.G., 1927. A contribution to the mathematical theory of epidemics. Proc. R. Soc. Lond. Ser. A Contain. Pap. A Math. Phys. Character 115 (772), 700–721.

King, A.A., Nguyen, D., Ionides, E.L., 2015. Statistical inference for partially observed Markov processes via the R package pomp. arXiv Prepr. arXiv 1509.00503.

Kraay, A.N.M., Hayashi, M.A.L., Berendes, D.M., Sobolik, J.S., Leon, J.S., Lopman, B.A., 2021. Risk for fomite-mediated transmission of SARS-CoV-2 in child daycares, schools, nursing homes, and offices. Emerg. Infect. Dis. 27 (4), 1229–1231. https://doi.org/10.3201/eid2704.203631.

Lanzas, C., Davies, K., Erwin, S., Dawson, D., 2020. On modelling environmentally transmitted pathogens. Interface Focus 10 (1), 20190056. https://doi.org/10.1098/rsfs.2019.0056.

Lee, E.C., Kelly Jr., M.R., Ochocki, B.M., Akinwumi, S.M., Hamre, K.E.S., Tien, J.H., Eisenberg, M.C., 2017. Model distinguishability and inference robustness in mechanisms of cholera transmission and loss of immunity. J. Theor. Biol. 420, 68–81. https://doi.org/10.1016/j.jtbi.2017.01.032.

Li, S., Eisenberg, J.N., Spicknall, I.H., Koopman, J.S., 2009. Dynamics and control of infections transmitted from person to person through the environment. Am. J. Epidemiol. 170 (2), 257–265. https://doi.org/10.1093/aje/kwp116.

Liang, M., Gao, L., Cheng, C., Zhou, Q., Uy, J.P., Heiner, K., Sun, C., 2020. Efficacy of face mask in preventing respiratory virus transmission: a systematic review and meta-analysis [Article]. Travel Med. Infect. Dis. 36, 101751 https://doi.org/10.1016/j.tmaid.2020.101751.

Nixon, E., Brooks-Pollock, E., Wall, R., 2021. Sheep scab transmission: a spatially explicit dynamic metapopulation model. Vet. Res. 52 (1), 54 https://doi.org/10.1186/s13567-021-00924-y.

Rohani, P., Breban, R., Stallknecht, D.E., Drake, J.M., 2009. Environmental transmission of low pathogenicity avian influenza viruses and its implications for pathogen invasion. Proc. Natl. Acad. Sci. USA 106 (25), 10365–10369. https://doi.org/10.1073/pnas.0809026106.

Teunis, P., Havelaar, A., 2000. The Beta Poisson dose-response model is not a single-hit model. Risk Anal. 20 (4), 513–520.

Towers, S., Chen, J., Cruz, C., Melendez, J., Rodriguez, J., Salinas, A., Yu, F., Kang, Y., 2018. Quantifying the relative effects of environmental and direct transmission of norovirus. R. Soc. Open Sci. 5 (3), 170602 https://doi.org/10.1098/rsos.170602.

Turner Jr, M.E., 1975. Some classes of hit-theory models. Math. Biosci. 23 (3–4), 219–235.

Van der Poel, W.H., 2014. Food and environmental routes of Hepatitis E virus transmission. Curr. Opin. Virol. 4, 91–96. https://doi.org/10.1016/j.coviro.2014.01.006.

Velkers, F.C., Bouma, A., Stegeman, J.A., de Jong, M.C., 2012. Oocyst output and transmission rates during successive infections with Eimeria acervulina in experimental broiler flocks. Vet. Parasitol. 187 (1–2), 63–71. https://doi.org/10.1016/j.vetpar.2011.12.032.

Velthuis, A., De Jong, M., Stockhofe, N., Vermeulen, T., Kamp, E., 2002. Transmission of Actinobacillus pleuropneumoniae in pigs is characterized by variation in infectivity. Epidemiol. Infect. 129 (1), 203–214. https://doi.org/10.1017/S0950268802007252.

Weber, T.P., Stilianakis, N.I., 2008. Inactivation of influenza A viruses in the environment and modes of transmission: a critical review. J. Infect. 57 (5), 361–373. https://doi.org/10.1016/j.jinf.2008.08.013.

Widgren, S., Bauer, P., Eriksson, R., Engblom, S., 2016. SimInf: an R package for data-driven stochastic disease spread simulations. arXiv Prepr. arXiv 1605.01421. https://doi.org/10.18637/jss.v091.i12.

Widgren, S., Engblom, S., Bauer, P., Frössling, J., Emanuelson, U., Lindberg, A., 2016. Data-driven network modelling of disease transmission using complete population movement data: spread of VTEC O157 in Swedish cattle. Vet. Res. 47 (1), 1–17. https://doi.org/10.1186/s13567-016-0366-5.

Widgren, S., Engblom, S., Emanuelson, U., Lindberg, A., 2018. Spatio-temporal modelling of verotoxigenic Escherichia coli O157 in cattle in Sweden: exploring options for control. Vet. Res. 49 (1), 78. https://doi.org/10.1186/s13567-018-0574-2.

Winther, B., McCue, K., Ashe, K., Rubino, J.R., Hendley, J.O., 2007. Environmental contamination with rhinovirus and transfer to fingers of healthy individuals by daily life activity. J. Med. Virol. 79 (10), 1606–1610. https://doi.org/10.1002/jmv.20956.

Woolhouse, M., 2011. How to make predictions about future infectious disease risks. Philos. Trans. R. Soc. B: Biol. Sci. 366 (1573), 2045–2054. https://doi.org/10.1098/rstb.2010.0387.